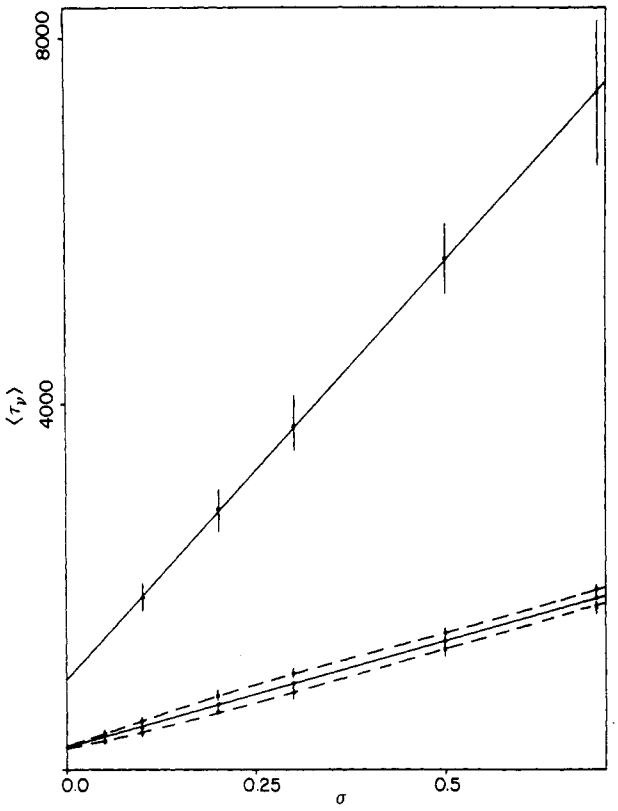

Figure 1. Plot of the longest average relaxation time of a random copolymer of 100 beads vs. the fraction σ of the second component. The solid line corresponds to the linear open chain while the broken curves correspond to the nondegenerate relaxation times of a ring copolymer. The vertical bars represent the error bars.

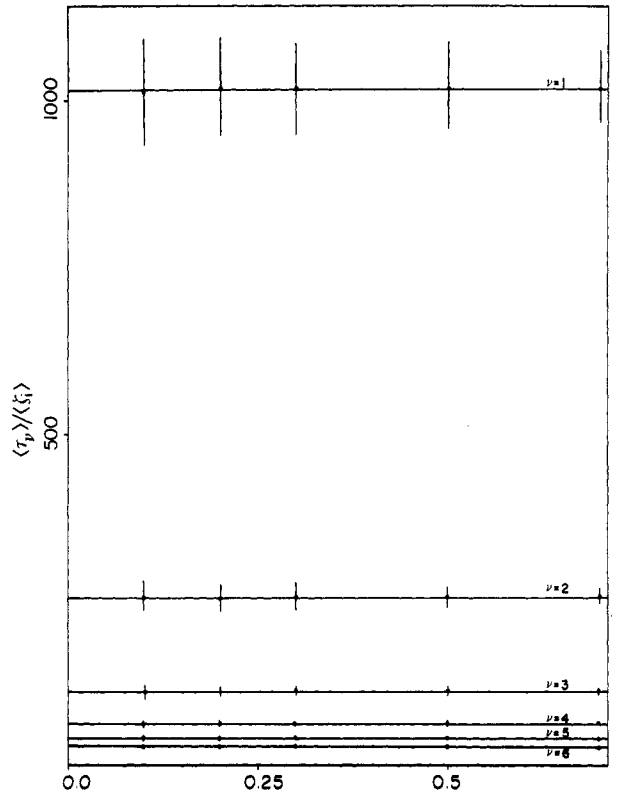

Figure 2. Plot of $\langle \tau_\nu \rangle / \langle \zeta_i \rangle$ for a linear copolymer against σ showing the proportionality of $\langle \tau_\nu \rangle$ to $\langle \zeta_i \rangle$ for all values of σ. ν = 1 is the longest lived mode.

be noticed in Figures 2 and 3 that the longest $\langle \tau_\nu \rangle$ for linear chains stays roughly proportional to 4 times the longest $\langle \tau_\nu \rangle$ of the ring case, for all σ values, due to the choice of

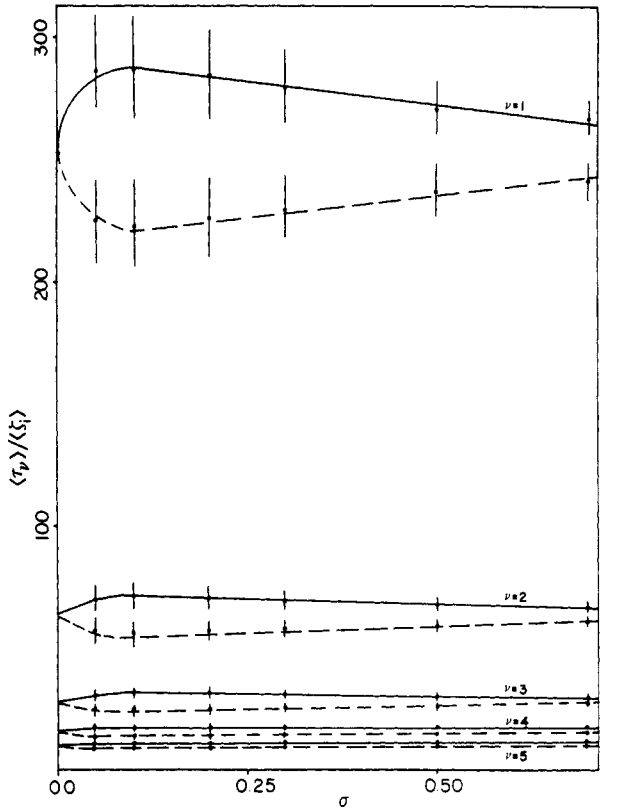

Figure 3. Plot of $\langle \tau_\nu \rangle / \langle \zeta_i \rangle$ for a ring copolymer vs. σ. The doubly degenerate modes of the uniform chain (σ = 0 or 1) split for 0 < σ < 1, the branches depending on σ nonlinearly. The average of these two branches is independent of σ.

the boundary conditions in diagonalizing the random matrix.

The n dependence of $\langle \tau_\nu \rangle \sim n^2$ is not affected by the introduction of the second component, although the eigenmodes are now no longer associated with the familiar Rouse modes of the uniform cases. Furthermore, as shown in Figure 2 and 3, $\langle \tau_\nu \rangle$ is proportional to $\langle \zeta_i \rangle$ and not to $\langle 1/\zeta_i \rangle^{-1}$, even though, $1/\zeta_i$ appears in the matrix of eq 2. This is in agreement with the conclusion reached in the recent mode coupling theory[4] of diffusion in stationary disordered media.

Acknowledgment is made to the National Science Foundation (Grant No. DMR-8403581) and the Materials Research Laboratory at the University of Massachusetts for support of this research.

References and Notes

(1) H. Yamakawa, "Modern Theory of Polymer Solutions", Harper and Row, New York, 1972.
(2) J. D. Ferry, "Viscoelastic Properties of Polymers", 3rd ed., Wiley, New York, 1980.
(3) K. F. Freed and S. F. Edwards, *J. Chem. Phys.*, **61**, 3626 (1974).
(4) J. Machta, M. H. Ernst, H. Van Beijern, and J. R. Dorfman, *J. Stat. Phys.*, **35**, 413 (1984).

^{13}C NMR Relaxation Study on Amylose in Dimethyl Sulfoxide

PHOTIS DAIS

Department of Chemistry, McGill University, Montreal, Quebec H3A 2A7, Canada. *Received November 12, 1984*

Interest in the motional behavior of polysaccharide molecules in solution has grown in recent years. In par-

0024-9297/85/2218-1351$01.50/0

Table I
Field Dependence of the ^{13}C Spin–Lattice Relaxation Times (ms) and NOE Values for Amylose in Me_2SO Solution at 80 °C

carbon	100 MHz	50 MHz	20 MHz
C-1	224 ± 10	127 ± 9	79 ± 6
	(1.58 ± 0.04)[a]	(1.90 ± 0.13)	(2.24 ± 0.08)
C-2–C-5	252 ± 15	150 ± 12	88 ± 8
	(1.64 ± 0.11)	(1.90 ± 0.10)	(2.12 ± 0.09)
C-6	152 ± 10	90 ± 8	62 ± 6
	(1.64 ± 0.08)	(2.02 ± 0.09)	(2.25 ± 0.09)

[a] Values in parentheses are the NOE values.

ticular, measurements of ^{13}C spin–lattice relaxation times have been carried out in several instances[1-4] for linear polysaccharides to probe variations in segmental motion for terminal groups and for branched polysaccharides to investigate differences in mobility between side-chain residues and those incorporated in the backbone. Experiments such as these have facilitated the assignment of ^{13}C resonance signals that were difficult to identify on the basis of chemical shifts and have provided a qualitative description of mobility, as reflected in the T_1 values. In this note, a quantitative treatment is presented of the molecular dynamics of a structurally homogeneous polysaccharide, namely, amylose, based on its ^{13}C spin–lattice relaxation characteristics.

Experimental Section

^{13}C-relaxation and NOE experiments were conducted with Bruker-400, Varian XL-200, and Bruker WP-80 spectrometers operating at 100, 50.03, and 20 MHz, respectively, for carbon-13 under broad-band proton decoupling. The probe temperature was 80 ± 0.5 °C.

The spin-lattice relaxation times were measured by the standard two-pulse recovery technique, adjusting the acquisition time so that the delay time between pulses was $AT \geq 5 \times T_1$. A total of 500–2000 acquisitions were accumulated for each set of 20–30 τ values. In general, τ values were chosen to cover approximately a $2 \times T_1$ range and "arrayed" in each run where possible. Values of T_1 were determined by a two-parameter fit using an equilibrium magnetization value that was the average of at least four separate determinations. The experiments were repeated until reproducibility of the data was better than 10% for the Bruker WP-80 and 5% for the other two spectrometers. The probable errors in the T_1 measurements from the two-parameter linear fit are shown in Table I.

^{13}C NOE measurements were carried out by "gating decoupling", three to five experiments being performed for each NOE value. Delays of at least 10 times the longest T_1 were used between 90° pulses. Samples of wheat starch amylose, 6% (w/v) in Me_2SO-d_6, were degassed by bubbling with nitrogen gas for 2 min before use. The molecular weight of amylose was 1.5×10^5.

Results and Discussion

The relaxation data (T_1 and NOE values) of amylose in Me_2SO at 80 °C and at three different frequencies are shown in Table I. The T_1 values for all protonated carbons increase with increasing field strength, reflecting the fact that the dynamics of amylose fall outside of the extreme narrowing limit. This is also indicated by the measured NOE values, which are less than the asymptotic value of 2.988 for simple highly mobile systems. These data constitute direct evidence for molecular motions occurring on a nanosecond time scale and, moreover, indicate that the simplest description of amylose dynamics by a single correlation time is not applicable.

It appears more appropriate to apply a correlation function corresponding to a distribution of correlation

Table II
Simulated Relaxation Parameters and Calculated Harmonic-Mean Correlation Times for Amylose in Me_2SO Solution at 80 °C

magnetic field, MHz	$s = 2$				$s = 3$				$s = 4$				$s = 5$			
	C-1		C-2–C-5		C-1		C-2–C-5		C-1		C-2–C-5		C-1		C-2–C-5	
	T_1[a]	NOE	T_1	NOE	T_1	NOE	T_1	NOE	T_1	NOE	T_1	NOE	T_1	NOE	T_1	NOE
100	224	1.88	250	1.99	230	1.84	252	1.98	227	1.70	258	2.05	224	1.66	250	1.99
50	148	2.19	172	2.38	127	1.99	158	2.03	127	2.02	151	2.10	126	2.00	152	2.18
20	100	2.72	126	2.83	70	2.07	98	2.41	61	2.08	83	2.06	65	2.18	79	2.10
τ_h, ns	0.29		0.22		0.55		0.25		0.77		0.35		0.83		0.42	

[a] In ms.

times,[5] indicating long correlation times associated with cooperative interactions between monomer units, as well as correlation times within the extreme narrowing region. Several alternative correlation functions of this form are available for treating the data. These models are characterized in general by two adjustable parameters, which reflect the distribution of correlation times and the width of this distribution. Mathematical functions used earlier for the analysis of relaxation data of polymers are the Cole–Cole,[6,7] Fuoss–Kirkwood,[8] and log (χ^2)[5,9] distributon functions. These functions, and in particular the log (χ^2) distribution, were able to account for ^{13}C T_1 and NOE data of some polymers, although the physical significance of the adjustable parameters has been questioned by other authors.[7b,10]

A second class of distribution functions has been generated by considering a three-bond crankshaft rearrangement in a chain embedded in a diamond lattice. There exist so far three modifications of this model depending on the boundary conditions involved in the solution of the lattice equation first derived by Hunt and Powles[11] from a different physical picture. These models[10,12,13] involving a distribution of correlation times have been successful in interpreting ^{13}C relaxation data for a number of polymeric compounds.[10,12,14] It may be noted that all these, more realistic, models yield quantitatively similar results when applied to a common data set, and the physical meaning of the model parameters is at least roughly similar.[15] Recently, Helfand et al.[16,17] developed a new correlation function for segmental motion based on computer simulation of chain dynamics. Although this new two-parameter function does not describe crankshaft conformational jumps, it led surprisingly to similar conclusions with the Jones–Stockmayer model in the interpretation of the segmental motion of polycarbonates.[18]

Under these circumstances, choosing the model that best describes polymeric dynamics is somewhat arbitrary. For convenience, the present relaxation data are quantified by using the "sharp cutoff" model of Jones and Stockmayer.[10] In this model, the parameters are the segment length $(2m - 1)$ or the parameter s $(=(m + 1)/2)$, which controls the breadth of the distribution, and the rate of occurrence w of the three-bond jump, usually expressed by the harmonic-mean correlation time $\tau_h = (2w)^{-1}$. The latter parameter reflects the distribution of correlation times.

Evaluaton of this model was done by computer solving eq 1, 2, and 16 of ref 10. The C–H bond distance was chosen to be 0.10 nm. A series of T_1 and NOE values were calculated with w in the range from 5×10^7 to 5×10^9 for a fixed s value. These computed values then were used to construct a family of relaxation curves (T_1 and NOE vs. log w) at the three magnetic field strengths employed. The most appropriate curve set (and hence w or τ_h and s values) was selected by obtaining the most consistent simulation of the relaxation-independent variables, i.e., T_1 and NOE's for C-1 and C-2–C-5 at these fields. The relaxation data for C-6 were not considered in this treatment, because this carbon lies outside the ring and is less hindered, and hence its relaxation receives additional contributions from rotational or oscillatory motion around the C-5,C-6 bond exocyclic to the ring.

The simulated relaxation parameters and calculated harmonic-mean correlation times obtained are shown in Table II. A satisfactory match of the experimental data over the three magnetic fields with $s = 2$, 3, 4, and 5 could not be obtained with the model adopted. Somewhat better agreement was obtained with a broader distribution ($s =$ 4 or 5), except for some of the simulated parameters; e.g., the T_1 of C-1 at 20 MHz was far removed from the observed value. However, the most serious deficiency of this model is the requirement of two harmonic-mean correlation times to describe the relaxation of two different carbon atoms in the same monomer unit (Table II). If the model is to be realistic it must accommodate such properties as, e.g., the fact that the ^{13}C relaxation times of two carbons in the same monomer unit depend exactly on the same autocorrelation function, if no particular angle dependencies of the C–H vectors are involved in the motional model.

The micro-Brownian motion of a polymer as described by the Jones–Stockmayer model implies that local motions should be accompanied by a relatively large conformational change along the main chain. However, this is not the case for amylose. Theoretical calculations[19,20] on amylose predict that the torsional angles ϕ and ψ, corresponding to energy minima, are constrained to a local region of only 1.5% of the conformational map. In addition, it has been suggested,[21] although not conclusively, that amylose in Me_2SO solutions behaves as a random coil with helical characteristics. This helical-like character of amylose may impose further restrictions on the local motions in the main chain.

In light of the present results, it appears more plausible that local conformational changes of amylose could be expressed as oscillatory, or other, types of motion within a disaccharide unit. These types of motions, whose amplitude depends on the constraints within the simple kinetic unit, introduce an angular dependence of the C–H dipolar interactions, a fact that may explain the difference in the relaxation times of C-1 and the remainder of the ring carbons. Consequently, additional theoretical calculations and experiments are envisaged in order to characterize the dynamics of amylose in terms of such possibilities. In this context, it is noteworthy that Kitamura et al.[22] have excluded the "lattice isomeric tetrahedral chain model" for amylose on the basis of fluorescence polarization data. On the other hand, a recent treatment[23] of the temperature-dependent ^{13}C relaxation data for amylose in Me_2SO at one field strength (15 MHz) using the "sharp cutoff" model resulted as well in two harmonic-mean correlation times for C-1 and the remaining ring carbons, respectively, although the author did not comment on this issue.

Acknowledgment. The author acknowledges the valuable assistance of Prof. A. S. Perlin in the preparation of this paper and thanks McGill University for financial support during the course of this investigation. The 100- and 20-MHz T_1 measurements were performed at the Laboratoire Regional de RMN à Haut Champ, Université de Montréal.

References and Notes

(1) Gorin, P. A. J. *Carbohydr. Chem. Biochem.* **1981**, *38*, 13.
(2) Perlin, A. S.; Casu, B. "The Polysaccharides"; Aspinall, G. O., Ed., Academic Press: New York, 1982; Vol. 1, Chapter 4.
(3) Seymour, F. R.; Knapp, R. D. *Carbohydr. Res.* **1980**, *81*, 67.
(4) Dill, K.; Allerhand, A. *J. Biol. Chem.* **1979**, *254*, 4524.
(5) Schaefer, J. *Macromolecules* **1973**, *6*, 882.
(6) Cole, K. S.; Cole, R. H. *J. Chem. Phys.* **1944**, *9*, 341.
(7) (a) Heatley, F.; Cox, M. K. *Polymer* **1977**, *18*, 225. (b) Heatley, F. and Begum, A. *Ibid.* **1976**, *17*, 399.
(8) Ghesquière, D.; Ban, B.; Chachaty, C. *Macromolecules* **1977**, *10*, 143.
(9) E.g.: Levy, G. C.; Axelson, D. E.; Schwartz, R.; Hochman, J. *J. Am. Chem. Soc.* **1978**, *100*, 410.
(10) Jones, A. A.; Stockmayer, W. H. *J. Polym. Sci., Polymn. Phys. Ed.* **1977**, *15*, 847.
(11) Hunt, B. I.; Powles, J. C. *Proc. Phys. Soc. London* **1966**, *88*, 513.
(12) (a) Valeur, B.; Jarry, J. P.; Geny, F.; Monnerie, L. *J. Polym.*

Sci., Polym. Phys. Ed. **1975**, *13*, 667. (b) Valeur, B.; Monnerie, L.; Jarry, J. P. *Ibid.* **1975**, *13*, 675. (c) Valeur, B.; Jarry, J. P.; Geny, F.; Monnerie, L. *Ibid.* **1975**, *13*, 2251.
(13) Bendler, J.; Yaris, R. *Macromolecules* **1978**, *11*, 650.
(14) E.g.: Heatley, F. *Prog. NMR Spectrosc.* **1979**, *13*, 47 and references therein.
(15) Jones, A. A.; Robinson, G. L.; Gerr, F. E. *ACS Symp. Ser.* **1979**, *No. 103*, 271.
(16) Hall, C. K.; Helfand, E. *J. Chem. Phys.* **1982**, *77*, 3275.
(17) Weber, T. A.; Helfand, E. *J. Chem. Phys.*, to be published.
(18) Connolly, J. J.; Gordon, E.; Jones, A. A. *Macromolecules* **1984**, *17*, 722.
(19) Jordan, R. C.; Brant, D. A.; Cesaro, A. *Biopolymers* **1978**, *17*, 2617.
(20) Brant, D. A.; Burton, B. A. "Solution Properties of Polysaccharides"; Brant, D. A., Ed.; American Chemical Society: Washington, DC, 1980; ACS Symp. Ser. No. 150, Chapter 7 and references therein.
(21) Winter, W. T.; Sarko, A. *Biopolymers* **1974**, *13*, 1447, 1461.
(22) Kitamura, S.; Tanahashi, H.; Kuge, T. *Biopolymers* **1984**, *23*, 1043.
(23) Matsuo, K. *Macromolecules* **1984**, *17*, 449.

Communications to the Editor

Synthesis and Two-Dimensional ^{19}F NMR of Highly Aregic Poly(vinylidene fluoride)

The free-radical polymerization of vinylidene fluoride (VF_2) is not completely regiospecific, so that the polymer PVF_2 contains occasional inverted or reversed monomer units as structural defects in an otherwise completely head-to-tail (isoregic) sequence.[1,2] The extent of reversed units depends weakly on temperature and varies over the limited range 3.5–6% under practical synthesis conditions.[3] This variation in defect content is too small to impart substantial differences in polymer properties. Therefore it would be desirable to have a series of PVF_2 samples with a much wider range of regioirregular monomer sequences to investigate structure–property correlations in detail, but heretofore such materials have been unrealized.

The structure of highly aregic PVF_2 may be approximated by introduction of the "pseudo" head-to-head ($-CF_2-CF_2-$) linkage by copolymerization of VF_2 with tetrafluoroethylene (F_4E).[4] However, VF_2–F_4E copolymers are not true regioisomers of PVF_2 in that they lack a tail-to-tail ($-CH_2-CH_2-$) linkage corresponding to each F_4E unit introduced.[5] The 1:1 alternating copolymer of ethylene with F_4E (e.g., Du Pont Tefzel) is a genuine regioisomer of PVF_2, but its structure is one extreme having 50% reversed units (syndioregic).

Our prior syntheses of PVF_2 have aimed at reducing the level of defects typically found in commercial materials. Thus we have achieved just 2.8% reversed units by deuterium labeling[6] and essentially the pure isoregic structure (i.e., no reversals) by the reductive dechlorination of poly(1,1-dichloro-2,2-difluoroethylene).[7] We now extend these studies to access the range of reversals above those in commercial samples. This report focuses on the novel synthesis of such materials and their characterization by fluorine-19 NMR.

Furthermore, by having PVF_2 samples with high (e.g., 18%) defect levels it is now feasible to perform two-dimensional *J*-correlated (COSY) experiments[8,9] and observe the connectivities between the signals from isoregic and aregic sequences. This experiment is extremely difficult with commercial PVF_2 where the aregic resonances are weak so that the 2D cross peaks are easily confused with artifacts generated by the intense ridges[8] radiating from the main isoregic peak. Fluorine-19 COSY spectra of commercial PVF_2 have been recorded but not published by Ferguson and Ovenall.[10] To date the only published 2D fluorine-19 homonuclear correlated experiment on polymers is the work on poly(vinyl fluoride) by Bruch et al.[11] Our present study with highly aregic PVF_2 has allowed us to verify in an absolute manner the main regiosequence assignments in the fluorine-19 NMR spectrum of PVF_2.

Scheme I

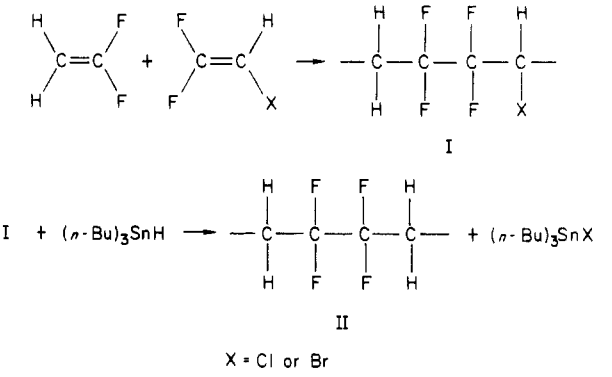

Our synthetic procedure is outlined in Scheme I. The precursor polymer I is made by copolymerization of VF_2 with either 1-chloro-2,2-difluoroethylene (CVF_2) or 1-bromo-2,2-difluoroethylene (BVF_2). We find that the chlorinated or brominated monomers are attacked at their CF_2 carbon by the growing $-CH_2CF_2\cdot$ radical, so that after reductive dechlorination or debromination with tri-*n*-butyltin hydride they become a reversed VF_2 unit in the final polymer II, which is therefore a regioisomer of PVF_2. A significant feature of the above scheme is the ability to control the level of reversed VF_2 units introduced via the comonomer units by varying the feed ratio in the initial copolymerization mixture.

Vinylidene fluoride was obtained from SCM Speciality Chemicals and purified by repeated freeze–degass–thaw cycles on a vacuum line after it had been passed through a column of silica gel for drying and removal of inhibitor. The comonomers BVF_2 and CVF_2 were also obtained from SCM and purified in an identical manner. The respective monomers were measured by their gas pressure in a calibrated volume and condensed in an ampule containing the initiator trichloroacetyl peroxide (TCAP), which was prepared and added as described previously.[6]

0024-9297/85/2218-1354$01.50/0